Thermal response of a closed loop pulsating heat pipe under a varying gravity force

M. Mameli [a,*], L. Araneo [c], S. Filippeschi [b], L. Marelli [c], R. Testa [a], M. Marengo [a,d]

[a] Università di Bergamo, Viale Marconi 5, 24044 Dalmine, BG, Italy
[b] Università di Pisa, DESTEC, Largo Lazzarino 2, 56122 Pisa, Italy
[c] Politecnico di Milano, Dipartimento di Energia, Via Lambruschini 4A, 20158 Milano, Italy
[d] School of Computing, Engineering and Mathematics, University of Brighton, Brighton BN2 4GJ, UK

Received 15 November 2013
Received in revised form
22 January 2014
Accepted 24 January 2014
Available online 4 March 2014

1. Introduction

Two-phase passive (or thermally driven) heat transfer devices, such as heat pipes and loop heat pipes, are currently the best available technology for the passive thermal control of electronics both in ground and in space conditions. In the early 90's a new concept of heat pipe, commonly known as Pulsating Heat Pipe (PHP), was introduced by Akachi [1]. It consists in a capillary channel with alternate heating and cooling zones, evacuated and partially filled with a working fluid. The thermal-hydraulic behavior mainly depends on the interplay between phase change phenomena (film evaporation, flow boiling, film condensation), capillary forces (able to maintain the fluid confinement in terms of slug/plug flow pattern) and gravity, which may assist or damp the fluid motion. Low cost, ease in manufacturing, compactness and outstanding features in terms of maximum heat transfer capability, thermal resistance, and temperature control make PHPs suitable for ground applications and promising for space applications. On the other hand the complex physical phenomena occurring inside the device (liquid film evaporation, fluid/wall interaction, flow pattern transition) are not fully characterized and the effect of several physical parameters on the device operation (number of heating/cooling sections, external acceleration field, geometry) is not yet clear.

In particular the inte rrelation between the effect of orientation with respect to gravity and the effect of the number of turns and/or heating and cooling sections is still a debated issue. The two effects have been investigated separately on ground: Yang et al. [2] showed that a relatively big number of heating and cooling sections (20 turns in the evaporator) coupled with a small internal diameter (1 mm) is beneficial in making the device operation almost independent from its orientation with respect to gravity, although the device had a particular, specific staggered layout and therefore no general conclusions are possible. Charoensawan and Terdtoon [3] investigated the thermal performance of horizontal closed loop PHPs with different number of turns (5, 11, 16, 26), internal diameters (1 mm, 1.5 mm, 2 mm), fluids (ethanol, water), evaporator lengths (50, 150 mm) and demonstrated that for a

* Corresponding author.
E-mail addresses: mcjmameli@gmail.com, mauro.mameli@unibg.it (M. Mameli).

Nomenclature

Bo	bond number [−]
d	diameter [m]
FR	filling ratio [−]
g	gravity acceleration [m/s^2]
Ga	Garimella number [−]
$\dot{Q}$	heat input power [W]
R	thermal resistance [K/W]
Re	Reynolds number [−]
T	temperature [°C]
U	fluid velocity [m/s]
We	Weber number [−]
μ	dynamic viscosity [Pa s]
ρ	density [kg/m^3]
σ	tension surface [N/m]

Subscripts

Bo	bond number
c	condenser zone
e	evaporator zone
eq	equivalent
Ga	Garimella number
l	liquid phase
max	maximum
min	minimum
Re	Reynolds number
v	vapor phase
We	Weber number

planar geometry with no gravity component in the flow path direction, the device with 5 turns never worked, and that the critical number of turns in order to achieve the device start-up is inversely proportional to the evaporator temperature and the inner diameter. Recently Mameli et al. [4] investigated the effect of orientation on the thermal performance of a perfectly planar CLPHP with 16 turns in the evaporator operated with FC-72 as working fluid. Despite the capillary inner diameter of 1.1 mm, the thermal resistance of the gravity assisted mode (bottom heated) performs more than two times better than the horizontal orientation. Probably, with a not negligible experimental effort, the coupled effect of inner diameter and thermal resistance could be better investigated with a systematic approach, even if one of the most common and fast solution for making the PHP independent on orientation in ground conditions is represented by designing three dimensional geometries [5,6], so that the device is partially assisted by gravity in any orientation. This approach is obviously not applicable when the acceleration field is absent (for example, for space applications): in this case the two effects must be investigated by creating an artificial microgravity environment (Drop Tower, parabolic Flight, Sounding Rockets) or by performing the experiments directly in orbit (for example, on the International Space Station). Gu et al. [7,8] performed experiments in normal, hyper (2.5g) and microgravity (0.02g aboard Falcon 20 aircraft flying parabolic trajectories) conditions on a Flat Plate Pulsating Heat Pipe (FPPHP) charged with R114, where square channels (1.5 mm) were engraved into an aluminum plate. One thermocouple was used to characterize the heating and cooling sections and the device is always tested in two positions: vertical gravity assisted or Bottom Heated Mode (BHM), vertical antigravity or Top Heated Mode (THM). They concluded that under reduced gravity, the heat pipes showed better operating and heat transport performances than under normal and hyper-gravity. By taking a careful look at the results in Ref. [7], the previous statement is supported by experimental evidence only for the top-heated mode. The occurrence of microgravity is naturally beneficial when the device is working in the antigravity mode, while the beneficial effect of microgravity is not evident against the top-heated gravity assisted PHP.

The present work aims at clarifying how a capillary tube PHP reacts to a variable acceleration field and proving that the thermal behavior of a symmetric 2-D PHP device working in the horizontal position on ground (no gravity component affects the internal axial fluid motion) is the most similar to the microgravity conditions, as suggested by the numerical simulations performed by Mameli et al. [9]. In Appendix A a further detailed discussion is offered to the reader in order to clarify the term “capillary tube” for the various gravity levels and the consequences in the choice of the PHP inner diameter.

A 2-D serpentine Closed Loop Pulsating Heat Pipe (CLPHP) made of a copper tube charged with FC-72 have been tested at different heat loads (up to 100 W), orientations (BHM, horizontal), transient gravity levels (0g, 1g, 1.8g). Beyond the standard thermal characterization and the hysteresis analysis on ground, an unprecedented experiment have been performed by changing the device orientation (vertical−horizontal−vertical) in order to obtain a gravity field variation with respect to the flow path direction and reproduce a (1g, 0g, 1g) gravity cycle. During the 58th ESA Parabolic Flight Campaign the device has been tested both in horizontal and vertical position throughout the parabola trajectory. The accuracy of the microgravity level obtained during the parabolic flight is ±0.05g.

The dynamic response of a symmetric 2-D PHP obtained during the ground tests shows interesting analogies to the dynamic response obtained during the microgravity tests.

2. Experiments

The pulsating heat pipe is made of a copper tube (I.D./O.D. 1.1 mm/2.0 mm) bended into a planar serpentine (32 parallel channels) where all curvature radii are 3 mm. Two “T” junctions allow to close the serpentine in a loop and to derive two ports at each side: one is devoted to the vacuum and filling procedure while the second one hosts a pressure transducer (Kulite®, ETL/T 312, 1.2bar A). The PHP is equipped with 14 “T” type thermocouples with wire diameter 0.127 mm, with an accuracy of ±0.1 °C after calibration; nine are tin soldered on the external tube surface in the evaporator and four in the condenser in order to maximize the thermal contact, a last one measures the ambient temperature. The test cell geometry as well as the thermocouple locations is shown in Fig. 1.

While evacuating the PHP by means of an ultra-high vacuum system (Varian® DS42 and TV81-T) down to 0.3 mPa, the working fluid (FC-72) is degased in a secondary tank by continuous boiling: incondensable gases accumulate un the upper part of the tank and they are sucked from above by means of several vacuuming cycles. Finally the PHP is filled with a volumetric ratio 0.5 ± 0.03 and permanently sealed by means of tin soldering. The incondensable gas content, less than 6 PPM, is estimated by measuring the difference between the actual fluid pressure inside the PHP and its saturation pressure at ambient temperature with the same procedure described by Henry et al. [13]. The present PHP is equipped with a wire electrical heater (Thermocoax® Single core 1Nc Ac, 0.5 mm external diameter) wrapped 20 times around each

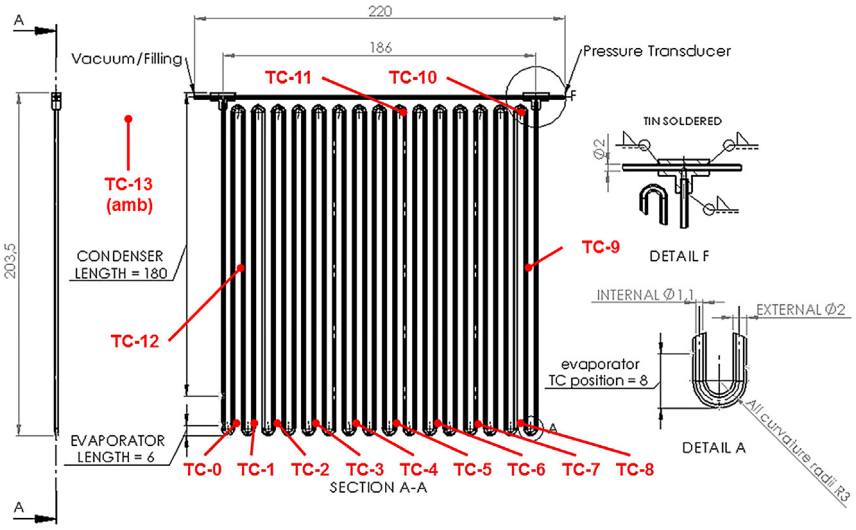

Fig. 1. Test-cell geometry and thermocouples location.

evaporator "U-turn" in order to cover an evaporator length of 6 mm, as shown in Fig. 2. Electric power up to 100 W is provided by a power supply (GWInstek® 3610A) corresponding to a radial heat flux up to 12 ± 0.3 W/cm^2. Thermal contact is obtained by heat sink compound.

This design allows minimizing the thermal inertia in the evaporator section, in order to avoid heat conduction between adjacent channels and to provide the same heating power to each "U-turn" in the evaporator. The PHP equipped with such a light heating system is able to reach the thermal pseudo-steady state in about 3 min. In this way the system is able to overcome transients before the beginning of each parabola sequence in order to obtain repeatable data (see Paragraph 3.3).

The condenser section is 180 mm long and it is cooled by means of a heat sink and air fan system. Circular cross section channels are milled on the surface of the aluminum heat sink so as to host the copper tubes. The PHP condenser is embedded into the heat sink (Fig. 3a) and fixed with an aluminum back plate. Thermal contact is obtained by heat sink compound. Four air fans are located on the heat sink fins in suction mode as shown in Fig. 3b. The PHP is equipped with a g-sensor (Dimension Engineering® DE-ACCM3D) located on one side of the heat sink. The test-cell (PHP, thermocouples, pressure transducer, g-sensor, heating and cooling system) is placed on a beam structure by means of four anti-vibration bushes. The structure may be fixed on the test rig plate with two different orientations: PHP vertical bottom heated, PHP horizontal. The thermocouples, the pressure transducer, the g-sensor, and the power supply are connected to a data acquisition system (NI-cRIO-9073, NI-9214®) and all signals are recorded at 16 Hz. The measurement parameters are:

- Heat input level: from 10 to 100 W with steps of 10 W. The corresponding wall heat fluxes are shown in Table 1.
- Orientation: vertical position heated at the bottom or Bottom Heated Mode (BHM); horizontal position.
- Gravity field: Normal gravity (1g) on ground and during the straight flying trajectory, hyper-gravity (1.8g) during the ascending and descending portion of the parabola, microgravity (0.01g) during the top portion of the parabola. Gravity fields different from normal gravity could be kept only for 20–22 s.

The measured quantities are:

- Temperature: external tube wall temperature is measured by means of 9 TCs in the evaporator and 4 TCs in the condenser; 1 TC for the environment.
- Pressure: one pressure transducer measuring the fluid pressure fluctuations in a single position within the condenser zone.
- Acceleration: a three-axis accelerometer allows monitoring the gravity field variation.

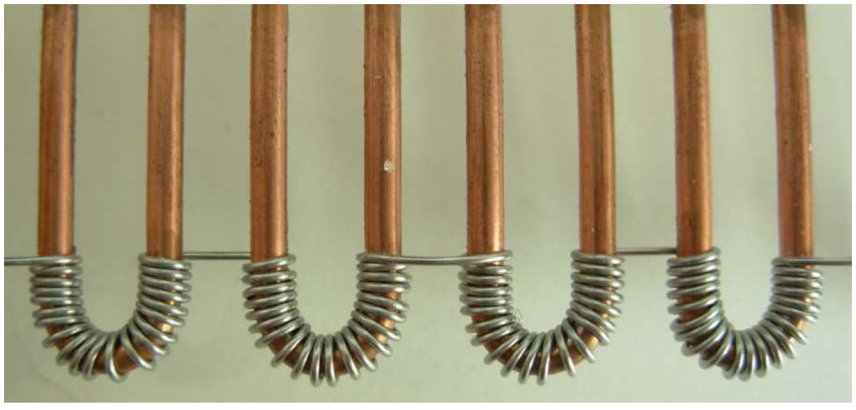

Fig. 2. Electric wire heating.

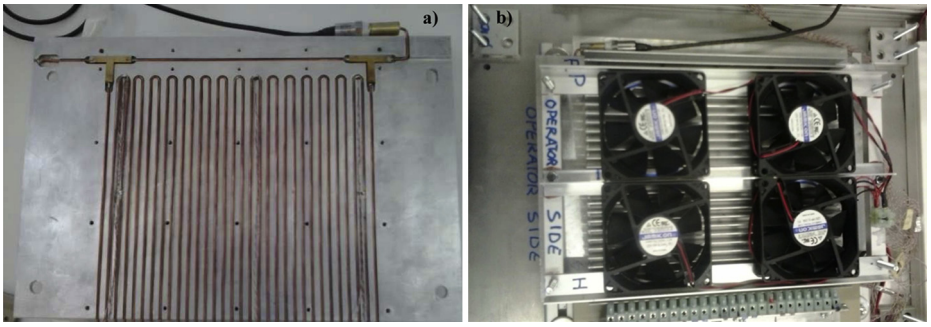

Fig. 3. a) PHP condenser section embedded into the aluminum heat sink; b) air fan system.

3. Experimental results

Results are presented mainly in terms of temperature and pressure time evolutions. In case of ground tests the secondary *y*-axis on the right reports the heat input levels during the thermal characterization, while the change in the orientation (0 = horizontal position; 1 = vertical) is plotted during the dynamic tests. In case of flight tests the secondary *y*-axis on the right reports the gravity acceleration. For the test cases, when a pseudo-steady state[1] has been reached, the equivalent PHP thermal resistance is also estimated at each heat input level using the temperature average.

3.1. Ground tests

Before the flight campaign, the device has been thermally characterized on ground (normal gravity condition) in vertical (Bottom Heated Mode) and horizontal orientation from 10 W to 100 W with steps of 10 W. Each heat input step is kept for 20 min even though the system is able to reach the pseudo-steady-state in about 180 s. In order to check the eventual dependency of the system on its "heating history", the characterization is performed also starting from 100 W down to 10 W. Repeatability tests have been performed both in the vertical and horizontal position starting from different heat input levels (20, 30, 40 W).

Vertical and horizontal orientations show very different behaviors confirming that, in a perfect 2D layout with a relatively high number of channels, gravity still plays an important effect on the PHP thermal behavior. Indeed in the horizontal working mode, the fluid motion is not assisted by gravity, oscillations are less frequent, the heat transfer rate is less efficient and, consequently, evaporator temperatures set to a higher value with respect to the vertical position.

Different working modes can be recognized during the vertical operation as shown in Fig. 4a: (i) the start-up mode; (ii) the standard operation and (iii) the thermal crisis.

3.1.1. Start-up mode

When the fluid pressure signal and temperature trends are starting to show fluctuations, but the pseudo-steady state has not yet reached, the device is said to run in the so-called start-up mode (SU = Start-up in Table 2). At low heat input levels the fluid motion is not well established and the heat transfer rate is not as effective as in the standard operation. Depending on the initial distribution of liquid slugs and vapor plugs, a very low heat input is not enough to start a vigorous and continuous fluid oscillation. As reported in literature [4,14] a critical minimum heat flux ($4 \div 5$ W/cm^2) is needed in order to start-up the device. Repeatability tests for the vertical position (Table 2) confirm that also for the present geometry the critical heat input is 30 W, equivalent to a radial heat flux of 3.51 W/cm^2. When the PHP is suddenly heated with the critical heat input, the start-up occurs and the device immediately settles to the standard operation regime, while if the device is initially heated with a lower heat input and the heat input gradually increases, the PHP start-up occurs only at 50 W (Fig. 4a).

3.1.2. Standard operation mode

When the start-up mode develops to a stable operation, temperatures and pressure are also able to reach a regular oscillating regime, called standard operation (ST = Standard Operation in Table 2). After the next heat input increasing, temperatures reach the pseudo-steady state after 3 min, and set in a narrow range (10 °C for the Vertical orientation and 20 °C for the horizontal orientation). Standard operation goes from the start-up heat input level (variable for the vertical orientation) to the occurrence of thermal instability or partial dry-out, where some channels undergo a fluid motion crisis and set to a much higher temperature.

3.1.3. Thermal crisis

The vertical operation shows an interesting feature at high heat input levels: some channels undergo a sudden thermal crisis probably due to fluid motion dampening or local dry-out [4]. In fact in case of heating-up (Fig. 4a) at 90 W only two thermocouples of nine are measuring a higher temperature in the evaporator, while at 100 W six channels are undergoing such thermal crisis. A similar trend is occurring in the heating-down case except a small hysteresis effect: since thermal crisis is active, it keeps occurring also at a lower heat input level (80 W), as detected by TC-2. Note that the total dry-out (all the channels are showing constant, very high temperatures) has not been reached for the present experimental test rig.

Finally the investigation shows that the partial dry-out is a gradual phenomenon: it starts with a thermal instability involving only a few channels which spreads throughout the remaining channels as the heat input increases. For practical applications the absence of a global sudden performance breakdown is a positive aspect, even if, on the other hand, such a wide temperature distribution due to thermal crunches is not desirable.

Table 1
Heat input power levels and corresponding wall to fluid heat fluxes.

Power [W]	10	20	30	40	50	60	70	80	90	100
Wall-to-fluid heat flux [W/cm^2]	1.17	2.34	3.51	4.69	5.86	7.03	8.20	9.38	10.55	11.72

[1] Pseudo-steady state is reached when all temperature signals show an average value constant in time.

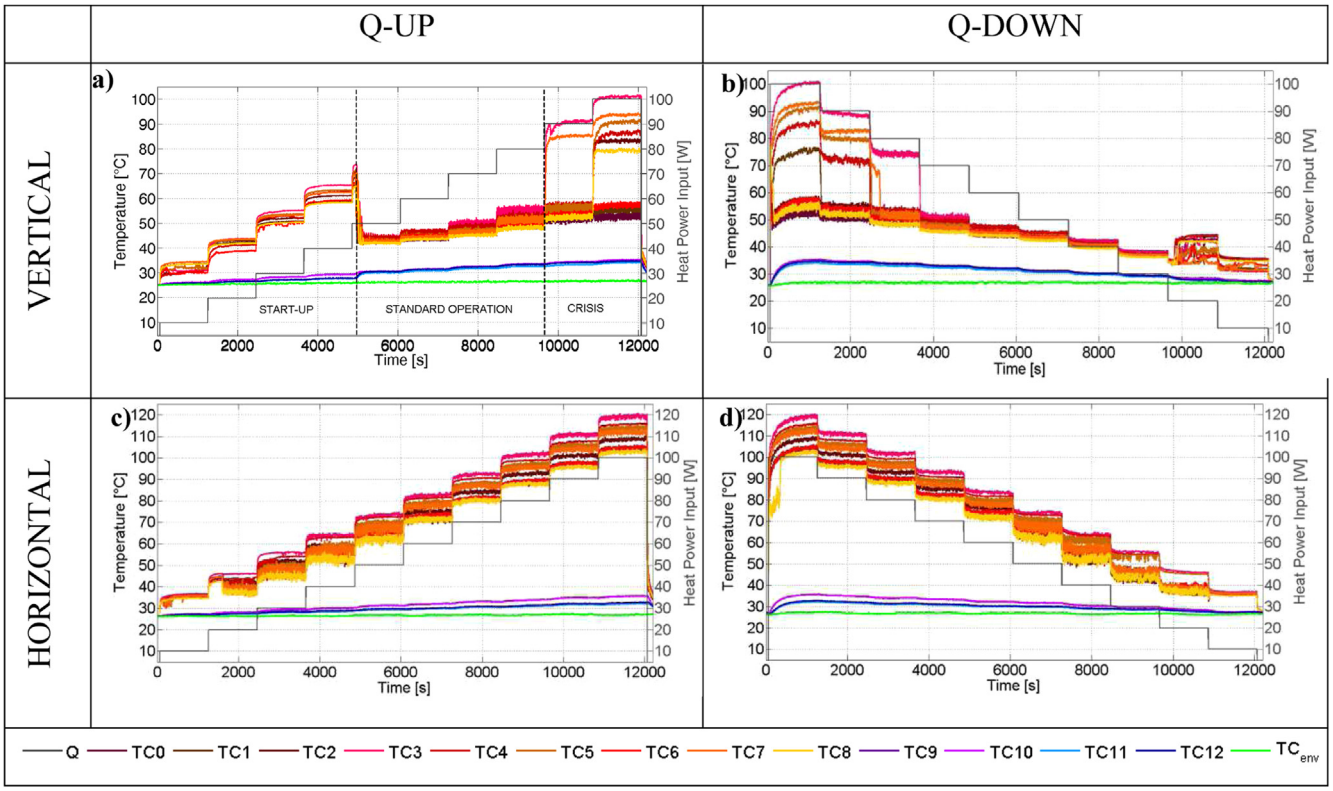

Fig. 4. Temperature evolutions during a steady thermal characterization on ground. Columns: increasing and decreasing the heat input; Rows: vertical and horizontal operation.

The horizontal operation does not show any sudden crisis in any of the channels, and the maximum temperature difference within the evaporator section (blue line in Fig. 5) is always between 10 °C and 20 °C without any step. For the vertical operation the temperature distribution is always very narrow during the standard operation (less than 10 °C), while it raises up to 50 °C when the crisis occurs.

The local pressure signal in the condenser is directly related to the flow motion and shows that the horizontal orientation operates with higher amplitude peeks with respect to the vertical orientation (Fig. 6a and b). Zooming on the steady state at 60 W, the vertical orientation confirms continuous oscillations, while the horizontal orientation reveals an alternation of short stop-overs and vigorous oscillations (Fig. 6c and d relatively). From the thermal point of view such impulsed driven flow leads the PHP evaporator to higher temperature levels with respect to the regular pulsating flow (Fig. 4). Despite the peeks in Fig. 6d seem to occur with a characteristic time rate, the Fast Fourier Transform analysis,

Table 2
Regime detection tests for the vertical operation (heating up mode).

VERTICAL	HEAT INPUT LEVEL [W]									
Test n°	10	20	30	40	50	60	70	80	90	100
1	NO	NO	NO	NO	SU/ST	ST	ST	ST	CR	CR
2	NO	SU	SU	SU/ST	ST	ST	ST	ST	CR	CR
3	NO	SU	SU/ST	ST	ST	ST	ST	ST	CR	CR
4	----	SU	SU/ST	ST	ST	ST	ST	ST	CR	CR
5	----	SU	SU	SU/ST	ST	ST	ST	ST	CR	CR
6	----	----	SU/ST	ST	ST	ST	ST	ST	CR	CR
7	----	----	SU/ST	ST	ST	ST	ST	ST	CR	CR
8	----	----	----	SU/ST	ST	ST	ST	ST	CR	CR
9	----	----	----	SU/ST	ST	ST	ST	ST	CR	CR
Legend. NO = No Operation; SU = Start-UP; ST = Stable Operation; CR = Thermal Crisis										

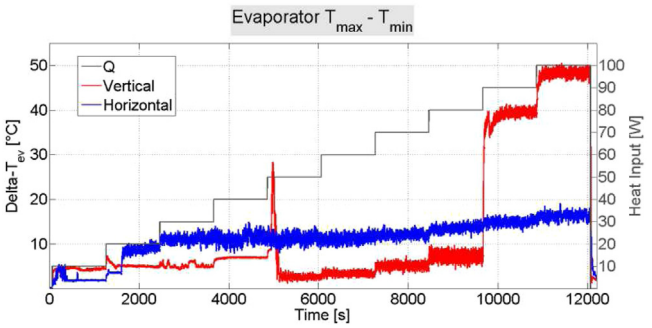

Fig. 5. Maximum temperature difference within the evaporator section for the vertical (red) and horizontal (blue) operation. (For interpretation of the references to color in this figure legend, the reader is referred to the web version of this article.)

performed on both signals (vertical and horizontal), does not indicate any dominant frequency (Fig. 6e and f).

Repeatability tests (Table 2) are performed starting from different heat input levels, namely 10, 20, 30, 40 W with the twofold aim of detecting the critical start-up heat input level and the occurrence of thermal instability. Table 2 eventually confirms that thermal crises occur at the same heat input level (90 W for the present PHP) for all the tests.

3.2. Dynamic response to the variable inclination

Beyond the steady thermal characterization, two dynamic investigations have been performed by changing the device orientation at a constant heat input level. The aim is to evaluate the transient time resulting from the change of orientation. Once the pseudo steady state is reached in BHM the device is suddenly tilted in the horizontal position, and let it there until the thermal equilibrium is reached again. Afterward the PHP is tilted back to the vertical position for another 20 s. The test has been repeated for three different heat input levels 50, 70 and 90 W. Fig. 7 shows the transient times needed to reach the new thermal equilibrium when the device is tilted from the vertical to the horizontal position (first column) and when the device is tilted back from the horizontal to the vertical position (second column). Note that when passing from the vertical to the horizontal position the device reaches a new pseudo-steady regime identical to the one reached during the standard horizontal test shown in Fig. 4.

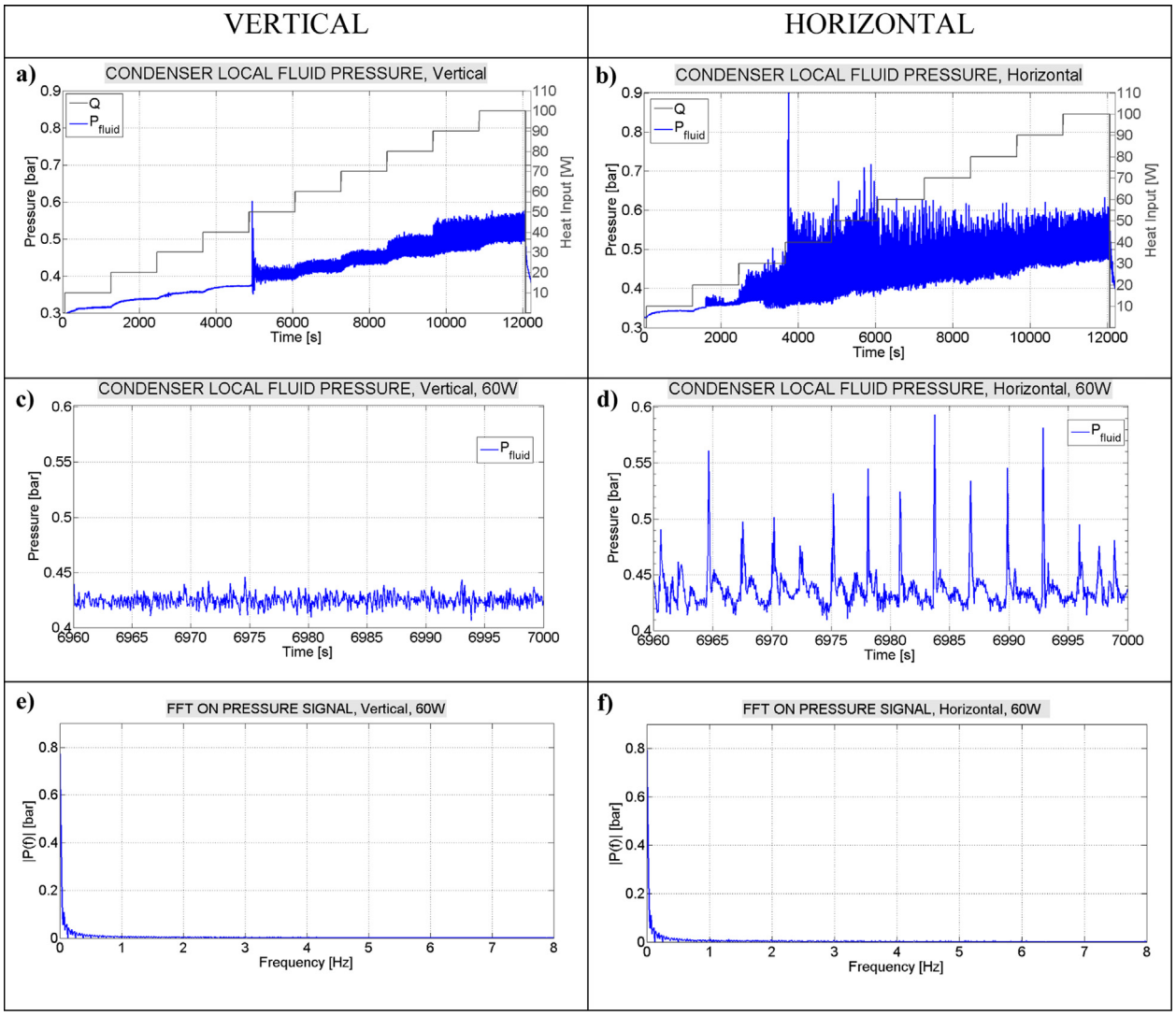

Fig. 6. Condenser local fluid pressure signal and power spectrum analysis in vertical and horizontal position.

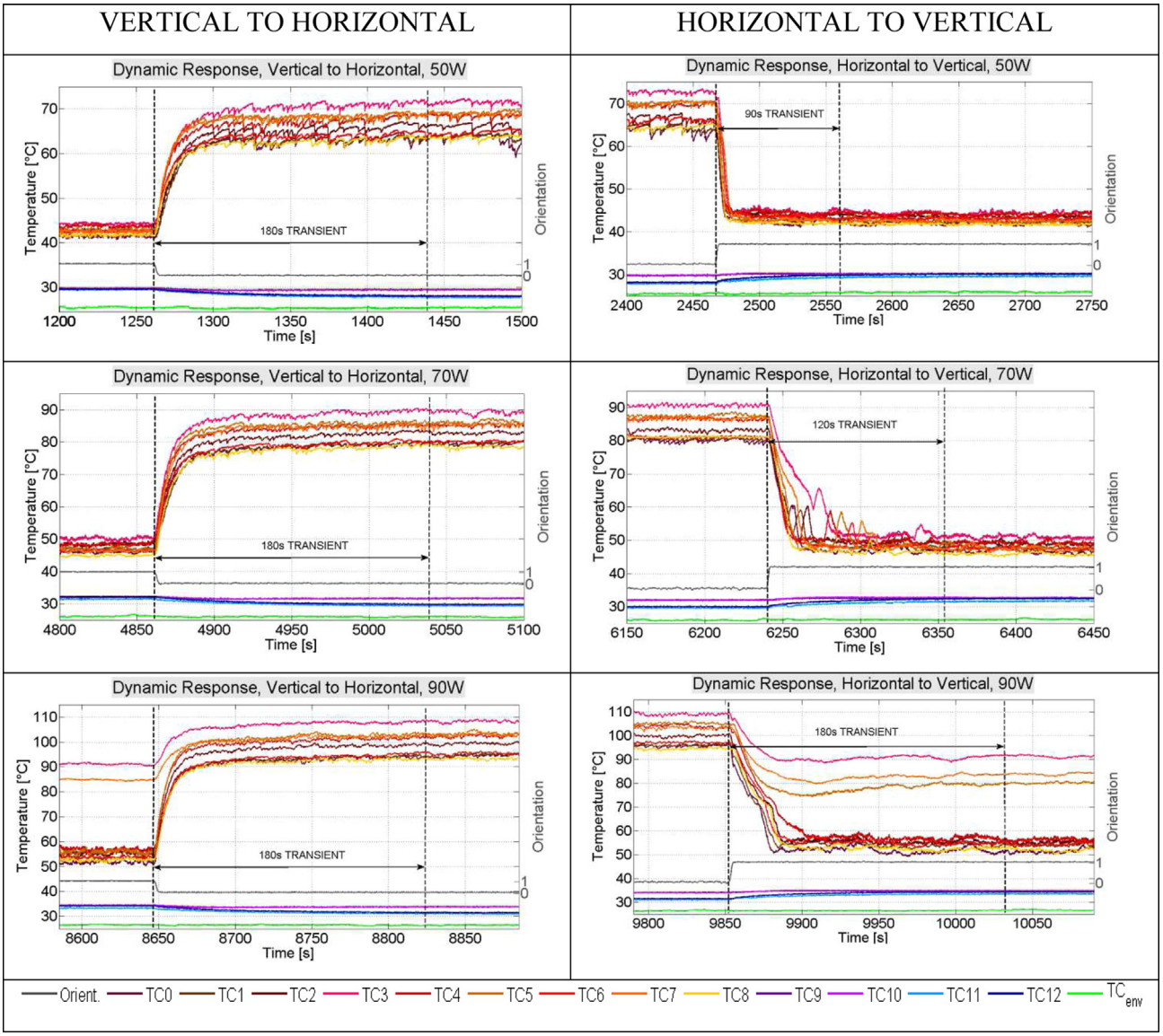

Fig. 7. Ground dynamic tests. First column: vertical to horizontal pseudo steady state reached in 180 s. Second column: horizontal to vertical.

Note that when the transient is done towards the unfavorable regime (from the vertical to the horizontal position) the transient time is 180 s while, if the transient is done towards a favorable regime (decreasing the heat input or from the horizontal to the vertical operation), the transient time is always shorter, even if it increases with the heat input level. The same test described above is performed by keeping the horizontal position only for 22 s, so as to obtain a gravity head variation with respect to the flow path direction, and reproduce a 1g to 0g to 1g, which is more similar to the gravity cycles during the parabolic flight. The device has been tested from 40 W to 100 W with steps of 10 W. Each heat input step is kept for 10 min in order to reach the pseudo steady condition, then the device is tilted in the horizontal orientation for 22 s then back again in the vertical position for 2 min. This dynamic sequence is repeated five times before changing to the next heat input level. The tests confirms once again that 20 s are not enough to overcome the transient, but they are still enough to provide clear data regarding the PHP dynamic response and to be compared with the data obtained by the flight tests as shown in the next sections. Data show perfect repeatability over the five maneuvers contained in the same heat input level.

3.3. Flight tests

The present experiment has been performed aboard the ESA/Novespace Airbus A300 in the framework of the 58th PF campaign. The PHP has been investigated both in horizontal and vertical position. Thirty-one parabolic trajectories are performed in each flight: the first one, called parabola zero, is followed by six sequences, each of five consecutive parabola. Five minutes at normal g-level are in between each sequence. The parabolic trajectory is

Table 3
Flight test procedure.

Parabola N.	PF-I (Vertical)	PF-II (Vertical)	PF-III (Horizontal)
0	Warm-up	Warm-up	Warm-up
1–5	40 W	100 W	50 W
6–10	50 W	90 W	60 W
11–15	60 W	80 W	70 W
16–20	70 W	70 W	80 W
21–25	80 W	60 W	90 W
26–30	90 W	50 W	100 W

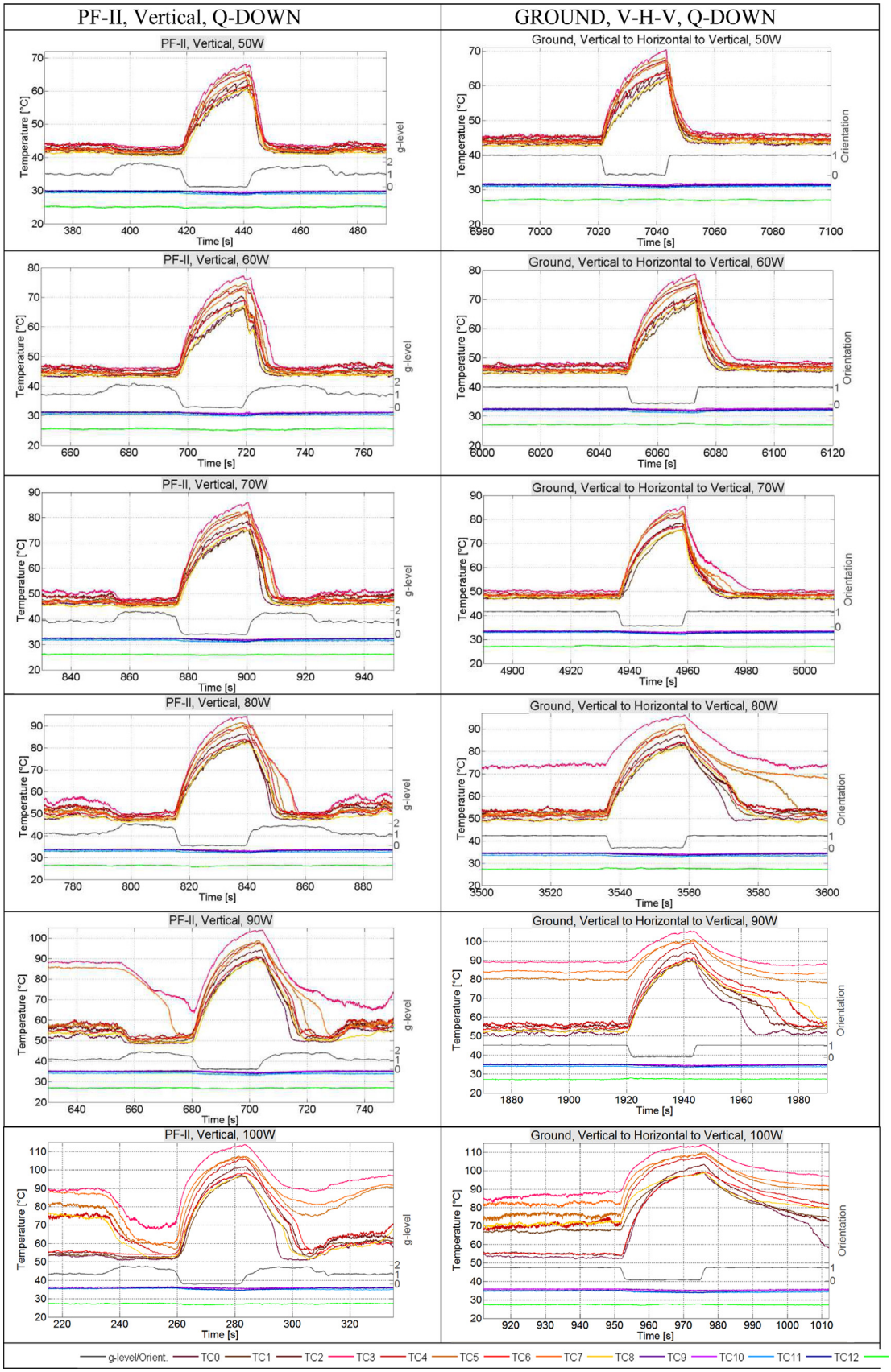

Fig. 8. Flight tests in vertical position compared with ground dynamic tests.

itself subdivided into three parts: 20 s at 1.8g (hyper-gravity) followed by 22 s at 0.01g (micro-gravity) followed again by 20 s at 1.8g (hyper-gravity). A 90 s pause of normal g-level flight is in between each parabola [15]. One flying day has been devoted to each of the three experiments resumed in Table 3, and called for sake of simplicity PF-I, PF-II, PF-III. As for the dynamic test on ground, the device has been tested from 40 W to 100 W with steps of 10 W. The heat input level is changed during the 5 min pause at normal g-level between each parabola sequence in such a way that the pseudo-steady state is reached at each heat input level before the beginning of the parabolic trajectories (1g 1.8g, 0g, 1.8g, 1g). The above strategy allows exploiting all the parabola and show that data are repeatable.

In the vertical position with the evaporator on the bottom in gravity conditions the acceleration field is in the channeled flow path direction, thus it gives a net contribution to the fluid momentum. For this reason both occurring of the hyper and the microgravity conditions are expected to affect the PHP thermal response. Since data show perfect repeatability over the five parabola at the same heat input level, the temperature temporal trend of only one single parabola is shown. In order to compare the dynamic response of the PHP in flight configuration and the PHP on ground during the Vertical to Horizontal to Vertical maneuver, also a single tilting operation is shown at the same heat input level. In case of flight tests the secondary *y*-axis shows the acceleration variation due to the parabolic trajectory while in case of ground tests shows the orientation (0 = Horizontal operation; 1 = Vertical operation).

Looking at Fig. 8 the effect of microgravity is evident for all the heat input levels: temperatures in the evaporator increase because the fluid motion is no more assisted by gravity, pressure oscillations are less frequent (Fig. 9a and b) and consequently the heat transfer rate is less efficient. The occurring of the second hyper-gravity period (last part of the parabolic trajectory) assists the fluid motion bringing back the device to the previous thermal regime. It is worth to stress the fact that the PHP fluid internal motion does not stop during the microgravity duration nor during the 20 s of horizontal tilting maneuver (Fig. 9a and b).

Since the effect of hyper-gravity is much less evident at low heat input levels, the thermal response to the absence of acceleration (0-g) looks very similar to the thermal response to the ground tilting maneuver (Horizontal). Note that during the ground maneuver, hyper-gravity is of course absent and the device is not able to recover the previous thermal regime as faster as during the flight experiments; the maximum temperatures reached by the evaporator during microgravity and during the horizontal period on ground are the same for all the heat input levels. This finally proves that the thermal regime of a planar PHP subjected to 20 s of microgravity environment is evolving to the same regime of a PHP operating on ground in horizontal position.

At 80 W the effect of hyper-gravity during the flight is strong enough to avoid the occurrence of thermal instability (clearly happening in the ground experiment, TC3). Increasing to 90 W the positive effect of hyper-gravity is even more evident: fewer channels undergo the thermal crisis. Finally at 100 W the augmented acceleration is not enough to avoid the occurrence of the thermal crunch, but still has a positive effect in recovering the previous thermal regime.

In the horizontal position the acceleration field is normal to the flow path direction. For this reason both hyper and microgravity conditions are not giving a net contribution to the fluid momentum along the channels and are not expected to greatly affect the PHP thermal response. The direct comparison between the flight data with ground experiments shown in Fig. 10 confirms that the variation of the acceleration field has no measurable effect on the PHP in the horizontal position.

3.4. Thermal resistance and repeatability

When the device is able to reach the pseudo-steady state at each heat input step it is possible to give an esteem of the overall thermal performance (equivalent thermal resistance). Thus the average temperature of the nine thermocouples located in the evaporator zone and the average temperature of the nine thermocouples located in the condenser zone can be calculated. Afterward, when pseudo-steady state is reached, the temperature time-average in the evaporator and the condenser is calculated. The overall equivalent thermal resistance is evaluated at each heat input step by the following equation.

$$R_{eq} = \Delta\overline{T}_{e-c}/\dot{Q}[K/W] \quad (1)$$

where $\Delta\overline{T}_{e-c}$ is the difference between the evaporator and the condenser average temperatures in the pseudo-steady state, and $\dot{Q}$ is the effective heat power input provided to the evaporator zone.

A hysteresis effect is observed during the vertical operation. Indeed, depending on the initial slug/plug distribution, if the PHP is heated up from a very low heat input, the induced vapor expansion may not be strong enough to start-up the device and the PHP inactivity can be prolonged till medium heat input levels are reached (see gray line in Fig. 11). On the other hand, if the PHP is heated at the maximum heat input since the beginning, start-up is immediately overcome and the device can keep the standard operation until the minimum heat flux for stable operation (30 W) is reached. Thermal resistance of a horizontal PHP does not show particular hysteresis effects and it is almost identical on ground and microgravity conditions confirming that gravity has no effects on a planar PHP positioned in the horizontal layout.

4. Conclusions

A multi-turn closed loop PHP with standard 2D geometry has been experimentally investigated on ground and in hyper/micro-

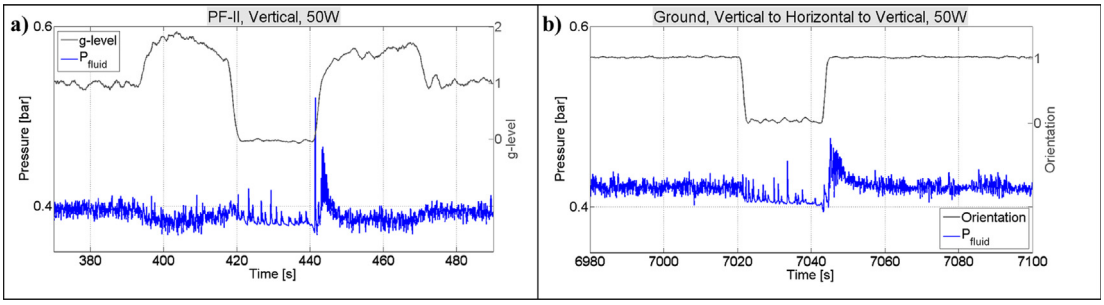

Fig. 9. Fluid pressure signal in the condenser section during a parabolic trajectory.

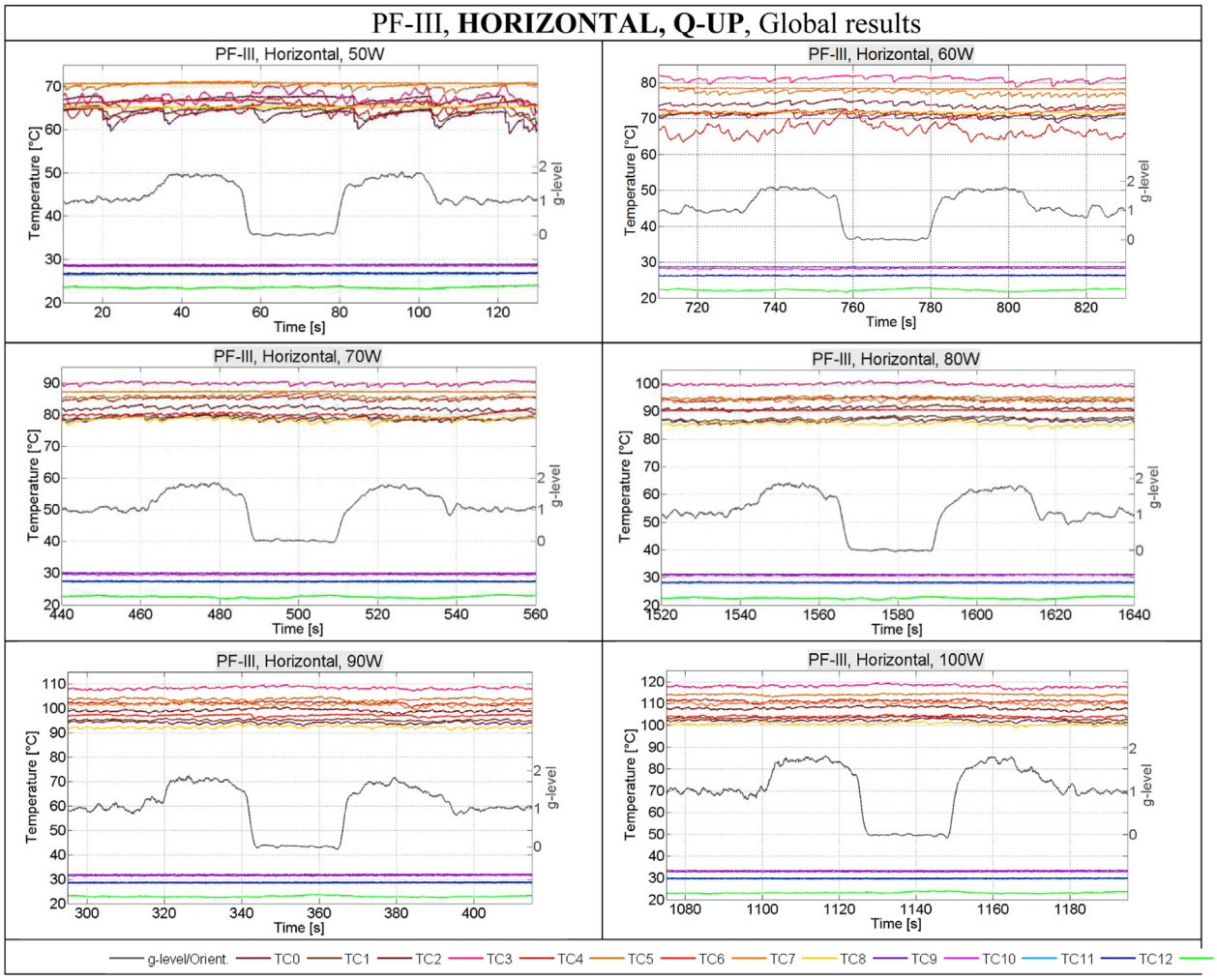

Fig. 10. Flight tests in horizontal position.

gravity conditions during the 58th ESA Parabolic Flight Campaign. The temporal trend of the wall temperature in several locations (evaporator and condenser) and the local fluid pressure signal show that the PHP thermal response is strongly and very rapidly affected by the variation of the gravity field. In particular the following salient points raise:

- The ground PHP operation is affected by the orientation with respect to gravity: the vertical operation with Bottom Heat Mode is more stable and efficient while the horizontal orientation is characterized by a pulsed flow with apparently lower oscillation frequencies.
- The vertical position is more dependent on the "heating history" than the horizontal position, showing a higher dependency on the initial conditions of liquid slug/vapor plug patterns before the power on. Furthermore a higher critical heat flux level is needed for the start-up of the bottom heated PHP.

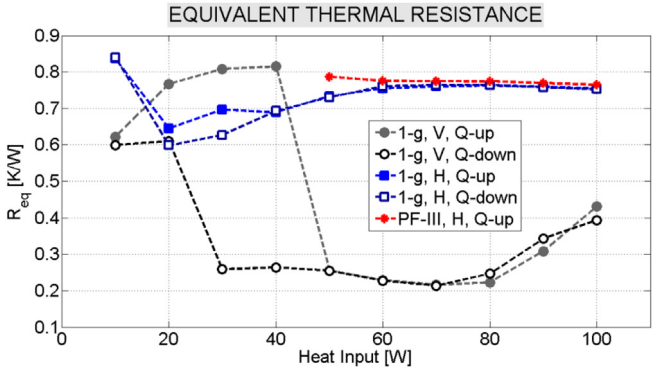

Fig. 11. Ground thermal characterization: Equivalent thermal resistance vs heat input.

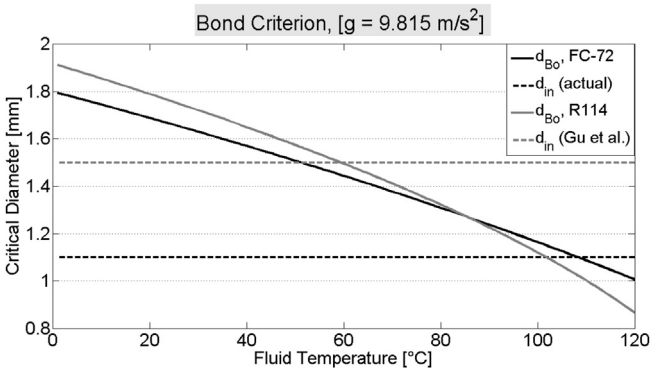

Fig. 12. Confinement diameter obtained with the Kew & Cornwell criterion [10] as function of temperature for refrigerants FC-72 and R114 and diameters used in the experiments.

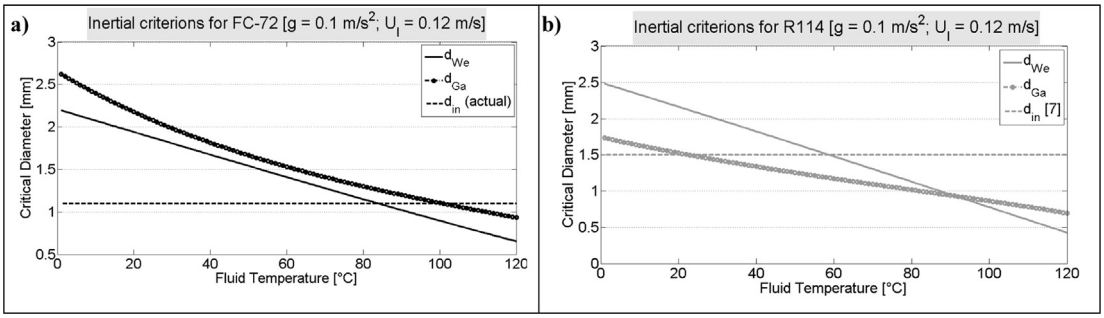

Fig. 13. Confinement diameter by Gu et al. [7] and Harichian & Garimella criterion [12] as function of fluid temperature for refrigerant FC-72 (a) and R114 (b).

- A repeatable thermal crisis is detected at high heat input levels for the vertical operation due to partial dry-outs. It revealed that the evaporator full dry-out is not a sudden event, but evolves gradually from the occurrence of the thermal instability by increasing the heat input level.
- The transient time needed by the present PHP to shift from the vertical to the horizontal running mode after a tilting maneuver is in the order of 180 s for all the heat input levels, thus 20 s are not enough to make statements on the PHP thermal performances, but only about its thermal dynamic response.
- During the parabolic flights (acceleration periodic sequence: 1g, 1.8g, 0g, 1.8g), only the vertical operation is affected by the gravity field variation: hyper-gravity slightly assists the flow motion, while during microgravity the PHP undergoes sudden temperature increase in the evaporator zone. The following hyper-gravity phase is able to bring the PHP back to the previous thermal regime.
- The thermal dynamic response to the occurrence of microgravity resembles the thermal dynamic response of a vertical-to-horizontal maneuver on ground.
- For a perfect 2D geometry, where in horizontal position the flow motion is never assisted by the gravity head, the horizontal operation on ground is the most similar to the microgravity operation.

Acknowledgments

The present work has been carried out in the framework of the Italian project PRIN2009 “Experimental and Numerical Analysis of Two-Phase Phenomena in Microchannel Flows for Ground and Space Applications” financed by MIUR and led by Prof. Marco Spiga, University of Parma. The authors acknowledge the financial support of the European Space Agency through the MAP Condensation program (AO-2004-096). A thanks is needed to NOVESPACE team in Bordeaux and to Dr. Vladimir Pletser from ESA for his support and encouragement in the parabolic flight campaign. The authors would like to thank Dr. Olivier Minster and Dr. Balazs Toth for their interest and support to the PHP activities and for the fruitful discussions. Finally we acknowledge all the members of the Pulsating Heat Pipe International Scientific Team, led by Prof. Marco Marengo, for their contribution in the pushing of the PHP technology for space applications, with a particular gratitude to Prof. Sameer Khandekar, Dr. Vadim Nikolayev and Dr. Vincent Ayel. Finally we thank Miriam Manzoni for her support in Bergamo and to have read and double-checked the final version of the manuscript.

Appendix A. On the fluid confinement in the PHP capillary tube

Since the device can be operated starting from normal gravity conditions, the fluid confinement criterion [10] based on the Bond Number must be satisfied in order to have an initial slug-plug pattern distribution: $Bo \leq 4$, where the Bond Number is defined as $Bo = g(\rho_l - \rho_v)d^2/\sigma$. So the critical diameter is calculated as follows

$$d_{Bo} \leq 2\sqrt{\frac{\sigma}{(\rho_l - \rho_v)\cdot g}} \tag{2}$$

Fig. 12 shows the confinement diameter obtained with Eq. (2) at different saturation temperatures with $g = 9.815$ m/s^2 for the refrigerants FC-72 and R114, this last fluid used by Gu et al. [7]. Physical properties are calculated with the NIST Refprop 8.0 [11].

In the present experiments the initial fluid temperature is less than 30 °C, and the Kew and Cornell criterion is largely satisfied, meaning that the slug/plug pattern is guaranteed as initial condition. The flow pattern may change at around 60 °C in the case of R114 and inner diameter of 1.5 mm, while the transition may occur at around 110 °C in the case of FC-72 and inner diameter of 1.1 mm. The experiments by Gu et al. [7] never exceed 60 °C, while the present experiment exceeds 110 °C at the maximum heat input (100 W) only in the horizontal position and during the microgravity period. After the start-up, the above criterion based on the Bond number alone may not be sufficient to define the fluid confinement, since also the fluid dynamics has clearly a role. If gravity acceleration is weak (microgravity) or absent (space environment), the Kew and Cornwell criterion has poor sense ($Bo \to 0$) and it could drive to the idea that a PHP could run in space with any diameter. As per the normal gravity operation, when heat power is provided to the evaporator zone, the fluid motion is activated and inertial and viscous effects are dominant over the capillarity effects depending on the liquid and vapor interfacial velocity. Furthermore the variation of the fluid physical properties with temperature properties cannot be ignored.

In order to account for the effect of inertia on the fluid confinement, Gu et al. [7] developed a basic model based on the ratio between kinetic energy and surface tension in order to determine whether the channel diameter is sufficiently small to maintain a plug/slug flow pattern in the PHPs under microgravity. The criterion can be finally expressed as a threshold of the liquid phase Weber number:

$$We_l \leq 4 \tag{3}$$

where $We_l = \rho_l U_l^2 d/\sigma$ is the Weber number related to the liquid phase. The critical diameter is the defined as:

$$d_{We} \leq 4\sigma/\rho_l U_l^2 \tag{4}$$

More recently Harichian and Garimella [12] developed a new semi-empirical transition criterion considering both inertial and viscous effects:

$$Ga = \sqrt{Bo} \times Re_l \leq 160 \quad (5)$$

where $Re_l = \rho_l U_l d/\mu_l$ is the Reynolds number related to the liquid phase. For sack of simplicity the number has been called Ga or Garimella number [10]. The critical diameter is then calculated as:

$$d_{Ga} \leq \sqrt{\frac{160\mu_l}{\rho_l U_l}} \sqrt{\frac{\sigma}{(\rho_l - \rho_v)\cdot g}} \quad (6)$$

Fig. 13a and b shows the confinement diameter respectively for FC-72 and R114 in a temperature range from 0 °C to 120 °C obtained with the Weber criterion (straight lines) and the Garimella criterion (spotted lines), assuming a fluid velocity of 0.12 m/s (on the basis of the visualization analysis carried on by Gu et al. [8]) and a gravity acceleration of 0.1 m/s^2. The actual diameters used in the present work (1.1 mm) and by Gu (1.5 mm) are also plotted as reference point. Despite a constant fluid velocity is not representative of the PHP operation (U_l depends on operating conditions and may cover a wide range), the present analysis gives a feeling that also in microgravity conditions the PHP diameter is still a critical issue.

In microgravity conditions the flow patterns inside the PHP are supposed to be confined (slug/plug regime) even when the tube diameter is bigger than the critical diameter, but a transition to semi-annular flow may occur due to inertial and/or viscous effects. This does not mean that the PHP is not able anymore to operate, but that its internal flow regime may change. Also in normal gravity conditions inertial and viscous effects should be taken into account: for instance, the Weber criterion suggests that the fluid in the present PHP (1.1 mm inner diameter, filled with FC-72) may undergo a flow pattern variation when its liquid temperature exceeds 80 °C assuming the constant fluid velocity of 0.12 m/s (Fig. 13). The transition would occur at higher fluid velocities for lower operating temperatures.

The present analysis reveals that a Closed Loop PHP could work under microgravity with slightly larger diameters with respect a capillary PHP on ground, but temperature working ranges must be carefully considered and analyzed. Further experimental and numerical investigations are needed in order to better determine the thermal responses for the different values of *Bo*, *We* and *Ga* numbers.

References

[1] H. Akachi, Structure of a Heat Pipe, US Patent 4,921,041, 1990.
[2] H.H. Yang, S. Khandekar, M. Groll, Operational limit of closed loop pulsating heat pipes, Appl. Therm. Eng. 28 (1) (2008) 49–59.
[3] P. Charoensawan, P. Terdtoon, Thermal performance of horizontal closed-loop pulsating heat pipes, Appl. Therm. Eng. 28 (2008) 460–466.
[4] M. Mameli, V. Manno, S. Filippeschi, M. Marengo, Effect of gravity on the thermal instability of a closed loop pulsating heat pipe, in: 8th World Conference on Experimental Heat Transfer, Fluid Mechanics, and Thermodynamics June 16–20, 2013, Lisbon, Portugal, 2013.
[5] S.M. Thompson, P. Cheng, H.B. Ma, An experimental investigation of a three-dimensional flat-plate oscillating heat pipe with staggered microchannels, Int. J. Heat Mass Transf. 54 (2011) 3951–3959.
[6] Y. Maydanik, V.I. Dmitrin, V.G. Pastukhov, Compact cooler for electronics on the basis of a pulsating heat pipe, Appl. Therm. Eng. 29 (2009) 3511–3517.
[7] J. Gu, M. Kawaji, R. Futamata, Effects of gravity on the performance of pulsating heat pipes, J. Thermophys. Heat Transf. 18 (3) (2004) 370–378.
[8] J. Gu, M. Kawaji, R. Futamata, Microgravity performance of micro pulsating heat pipe, Microgravity Sci. Technol. 16 (2005) 181–185.
[9] M. Mameli, M. Marengo, S. Zinna, Numerical investigation of the effects of orientation and gravity in a closed loop pulsating heat pipe, Microgravity Sci. Technol. Int. J. (2012), http://dx.doi.org/10.1007/s12217-011-9293-2.
[10] C. Baldassari, M. Marengo, Flow boiling in microchannels and microgravity, Prog. Energy Combust. Sci. 39 (1) (February 2013) 1–36.
[11] E.W. Lemmon, M.L. Huber, M.O. Mclinden, NIST Standard Reference Database 23: Reference Fluid Thermodynamic and Transport Properties-refprop, Version 8.0, National Institute of Standards and Technology, Standard Reference Data Program, Gaithersburg, 2007.
[12] T. Harichian, S. Garimella, A comprehensive flow regime map for microchannel flow boiling with quantitative transition criteria, Int. J. Heat Mass Transf. 53 (2010) 694–702.
[13] C.D. Henry, J. Kim, B. Chamberlain, Heater size and heater aspect ratio effects on sub-cooled pool boiling heat transfer in low-g, in: 3rd International Symposium on Two-phase Flow Modeling and Experimentation Pisa, 22–24 September 2004.
[14] M. Mameli, M. Marengo, S. Khandekar, Local heat transfer measurement and thermo-fluid characterization of a pulsating heat pipe, J. Therm. Sci. 75 (2014) 140–152.
[15] Novespace A300 Zero-G Rules and Guidelines, April, 7th 2009. RG-2009-2, NOVESPACE 15, rue des Halles 75001 Paris – France.